

Backward emitted high-energy neutrons in hard reactions of p and π^+ on carbon

A. Malki^a, J. Alster^a, G. Asryan^{c,b}, D. Barton^c, V. Baturin^{e,d}, N. Buchkojarova^{c,d}, A. Carroll^c, A. Chtchetkovski^{e,d}, S. Heppelmann^e, T. Kawabata^f, A. Leksanov^e, Y. Makdisi^c, E. Minina^e, I. Navon^a, H. Nicholson^g, Yu. Panebratsev^h, E. Piassetzky^a, S. Shimanskiy^h, A. Tangⁱ, J.W. Watsonⁱ, H. Yoshida^f, D. Zhalov^e

^a*School of Physics and Astronomy, Sackler Faculty of Exact Sciences, Tel Aviv University.* ^b*Yerevan Physics Institute, Yerevan, Armenia.* ^c*Brookhaven National Laboratory.* ^d*Dept. of Physics, St. Petersburg Univ., St. Petersburg, Russia.* ^e*Physics Department, Pennsylvania State University.* ^f*Dept. of Physics, Kyoto Univ., Kyoto, Japan.* ^g*Mount Holyoke College.* ^h*J.I.N.R., Dubna, Russia.* ⁱ*Dept. of Physics, Kent State University.*

Abstract

Beams of protons and pions of 5.9 GeV/c were incident on a C target. Neutrons emitted into the back hemisphere, in the laboratory system, were detected in (triple) coincidence with two emerging $p_t > 0.6$ GeV/c particles. We present the momentum spectra of the backward going neutrons, which have the same universal shape observed in earlier (inclusive) reactions induced by hadrons, γ , ν , and $\bar{\nu}$ beams. We also integrated the spectra and determined the fraction of the hard scattering events which are in coincidence with at least one neutron emitted into the back hemisphere, with momenta above 0.32 GeV/c. Contrary to the earlier measurements which found that only a small fraction (of the order of 10%) of the total inelastic cross section for light nuclei was associated with backward going nucleons, we find that about half of the events are of this nature. We speculate that the reason for the large difference is the strong total center of mass (s) dependence of the hard reaction and short range nucleon correlations in nuclei.

PACS: 21.30.-x, 25.40.-h, 24.50.+g

There has been an intensive experimental program directed toward the systematic characterization of the emission of backward going nucleons from nuclei in collisions with high energy (> 1 GeV) hadrons [1, 2, 3, 4], real photons [5], virtual photons [1], neutrinos and antineutrinos [6, 7, 8]. In these experiments the nucleons were emitted into angles larger than 90° in the laboratory system. Thus, the kinematical conditions were such that the observed backward nucleon could not result from a single two-body scattering of the incident particle with a nucleon at rest in the nucleus. Even though these experiments involved a large variety of interactions, energies and nuclei, a common universal spectrum of the backward nucleons was observed. This spectrum can be parameterized by the expression:

$$(E/p) \frac{d\sigma}{d(p^2)} = C e^{-Bp^2} \quad (1)$$

where E and p are the energy and momentum of the backward going nucleon.

For incident beams above about 1 GeV/c and for backward going nucleons above about 0.3 GeV/c the slope parameter B was found to be independent of incident energy and beam type and target nucleus and only weakly dependent on the angle of the backward going particle (see below for details). The absolute scale parameter C depends on the nucleus and only weakly on the incident energy and projectile. The fraction of high energy (above the Fermi sea level) backward nucleons with respect to the total inelastic events for light nuclei (C, Ne) is of the order of 10% (see Table I).

In this paper we present the first measurement of high energy backward neutrons emitted from a nucleus *in coincidence with two high- p_t particles*, ($p_t > 0.6$ GeV/c). We find that, while the universal shape of the momentum spectra is maintained, the measured fraction of events with two high p_t particles in coincidence with a backward going neutron is substantially higher than the ratios measured for the more inclusive reactions. A detailed description of our experiment follows.

We present the first results from a measurement which was performed during 1998 with the rebuilt EVA spectrometer at the AGS accelerator of Brookhaven National Laboratory. The spectrometer consisted of a superconducting solenoidal magnet operated at 0.8 Tesla (see Fig. 1). The scattered particles were tracked by 4 sets of 4-layer straw tube cylindrical drift chambers (not shown) which surrounded the beam axis cylindrically. These straw tubes measured the transverse momenta of the particles by drift time

and the polar scattering angle by charge division. Details on EVA spectrometer straw tube system are given in refs. [9, 10, 11, 12]. The major change to the spectrometer in addition to the improved performance of the solenoid and straw tubes was the installation of two new neutron counter arrays which increased the acceptance by a factor of 2.5 over the 1994 configuration [13].

At a momentum of 5.9 GeV/c the beam consisted of about 40% protons and 60% pions, identified by a sequence of two differential Cerenkov counters. The beam entered along the symmetry axis (z) of the magnet with an intensity of $\approx 1 \times 10^7$ particles over a one second spill, every 3 seconds. A scintillator hodoscope in the beam served as timing reference. Three solid targets consisting of various combinations of CH₂ and C were placed on the z axis, separated by about 20 cm. They were 5.1×5.1 cm² wide and 6.6 cm long in the z direction. Their positions were interchanged several times at regular intervals. Some of the runs were with three C targets and some with two C targets and one CH₂ target.

As indicated in Fig 1, we triggered the spectrometer on two positively charged particles which emerged from the downstream end of the solenoid at polar angles of $(27.5 \pm 3)^\circ$ which corresponds to about 90° in the pp center of mass. For this analysis, events with two particles with a $p_t > 0.6$ GeV/c which originated from one of the C targets were selected. The trigger required that one particle go to the left of the beam, and the other to the right. In addition we required that there were no additional charged tracks in the straw tubes. The polar angle coverage of the inner straw tube cylinder extended from about 10° to 150° . Three scintillator arrays measured the direction and energy of neutrons, in coincidence with these two particles.

In Fig. 1 we present a schematic picture of the setup. We show the magnet of the EVA spectrometer and the positions of the targets. Below the targets we placed a series of 12 scintillator bars (ARRAY 1 in Fig. 1) covering an area of 0.6×1.0 m² and 0.25 m (2 layers 0.125 m each) deep. They spanned a polar angular range of 84° to 110° and an azimuthal range from 165° to 195° . A similar array of 16 scintillator bars (ARRAY 2), covering an area of 0.8×1.0 m² and 0.25 m deep, spanned a polar angular range of 110° to 132° and the same azimuthal range as the first one. Each individual counter in these two arrays was $10 \times 12.5 \times 100$ cm³ in size and had a 5.1 cm photomultiplier at each end. The third array (ARRAY 3) was constructed from one layer of eight $10 \times 25 \times 100$ cm³ counters with a 12.7 cm photomultiplier at each end. This third array covered an area of 2.0×1.0 m² and spanned

a polar angular range of 72° to 120° and an azimuthal range from 120° to 150° . A set of veto counters (not shown in Fig 1.) served to discriminate against charged particles. Lead sheets (not shown in Fig 1.) with a total thickness of 1.7 radiation lengths were placed in front of the veto counters in order to reduce the number of photons entering the time of flight (TOF) spectrum. All counters were set to an electron equivalent detection threshold of 1 MeV by fixing a discriminator at the Compton edge of a ^{60}Co gamma source. This procedure is similar to the description in ref. [14]. The detection efficiency was determined by the Monte Carlo method described in ref [15]. The efficiencies depend on the neutron momentum and they ranged from about 30% at 0.15 GeV/c to about 15% at 0.5 GeV/c, for a typical single counter. We considered only neutrons above 0.15 GeV/c to avoid large uncertainties in the efficiency calculations of the neutrons at low momenta. A fraction of the neutrons gets absorbed on the trajectory from the target to the counters. The probability that a neutron was removed was calculated by assuming that the removal cross section was equal to the non-elastic cross sections in the materials [16]. We assigned an uncertainty of 25% to these removal cross sections. The attenuation depends on the neutron momentum and the values ranged from about 35% at the low momenta to about 20% at the high momenta. The neutron momenta were determined from their TOF. A clearly identified peak due to remaining photons from the targets was used for calibration and to measure the timing resolution. That resolution was $\sigma \leq 1$ ns which corresponds to a momentum resolution of $\sigma = 30$ MeV/c at the highest momentum (0.5 GeV/c). We applied a cut in the TOF spectrum at 7 ns/m, keeping neutrons below 0.5 GeV/c, in order to eliminate the remaining photons.

In Fig 2. we present the measured invariant momentum spectra $(E_n/p_n) \times \frac{N_3}{d(p_n^2)}$ in arbitrary units for pion and proton incident beams, where E_n and p_n are the energy and momentum of the neutron detected in the backward hemisphere ($90^\circ < \theta_n < 130^\circ$) and N_3 is defined below. We call N_2 the number of events with two high transverse momentum charged particles with $p_t > 0.6$ GeV/c, each and no other charged particles seen in the detector. We applied software cuts to allow better determination of the target position from the track reconstruction and to obtain a better separation between incident protons and pions. The number of triple coincidence events which fulfill all the conditions of the N_2 events and, in addition, have a single neutron in the scintillator bars is indicated by N_3 . Since the efficiency and

attenuation corrections depend on the neutron momentum they were done event by event. The resulting spectra are plotted on a semi-logarithmic scale as a function of p_n^2 . The error bars represent the statistical errors only. The curves above $p_n^2 > 0.1$ (GeV/c)² were fitted to a first order polynomial. The slope parameters (B in equation 1) for the proton and pion incident beams are shown in the figure with their fitting error. For comparison we quote the slope parameter obtained from the p+C→ n+X data [3] at 7.5 GeV/c. Their value at 119°, which lies within the range of our measurement, is $B=13.0\pm 0.8$ (GeV/c)⁻². The neutrino measurements [6, 7, 8] report a value of $B=9.5-10.7$ (GeV/c)⁻² for protons emitted into the whole backward hemisphere with uncertainties ranging from 0.3 to 2 (GeV/c)⁻². Ref. [6] presents a compilation of other experiments at several different energies of hadron and photon beams incident on a variety of targets, including C and other light nuclei. For particles in the common angular range of 120°-150° of the different experiments, the slope parameters all lie within the range of 10-12.5 (GeV/c)⁻² with a typical error of 2 (GeV/c)⁻². Our first conclusion is that the slopes we measured in this experiment agree, within the measured uncertainties, with the slopes obtained using hadrons, photons and neutrino beams of different energies incident on various targets. The angular ranges are not the same for all experiments but this does not modify the values of B sufficiently to affect the conclusion (see [8]).

We also wish to compare our yield of backward scattered neutrons above 0.32 GeV/c to those of the other experiments. In Fig. 3 we show the (triple coincidence) backward yield per unit solid angle divided by the (double coincidence) two high- p_t particle yield vs. the neutron angle. Each point in this figure contains 10-20 combinations of target positions and a neutron-counter (with the exception of the most forward angle point which includes 3 such combinations only). The errors in the figure are the statistical errors combined with up to 10% systematic errors due to software cuts, uncertainties in the neutron detection thresholds and uncertainties related to determining the exact geometrical positions of the counters. To obtain the yield into the backward hemisphere we fitted the ratios to a constant (see fig 3). For the proton induced reaction this gives a value of $(7.4\pm 0.4)\%$ /sr and for the pion induced reaction the value of $(6.5\pm 0.6)\%$ /sr above 90° and 100°, respectively where the ratios become constant. We used the parameters of the fit to extrapolate up to $\theta_n = 180^\circ$, assuming that the ratio remains constant. The results for the pion and proton induced reactions are shown in Table 1 com-

pared with the earlier mentioned experiments. Our results are given for the integration up to $\theta_n = 130^\circ$ with the proper error as well as for the integration to $\theta_n = 180^\circ$ which assumes the constant ratio out to that angle. Our second conclusion from this experiment is, that in this measurement the ratio is substantially larger (3-4 times) than for the more inclusive measurements. This is true even if we include only our yield out to $\theta_n = 130^\circ$. Integrating out to 180° can only increase that ratio.

The earlier experiments have led to several theoretical interpretations. The models that have been discussed can be divided into two main classes. The first class [17, 18, 19, 20] deduces from the universality that the measurement must provide direct information on the nuclear ground state, especially on the high-momentum part of the wave function. These models assume that the projectile interacts with a single nucleon and that the backward yield of nucleons is due to the break-up of pre-existing two, or more, correlated nucleon clusters [17, 18]. One of the more extreme models in this class assumes that the high momentum of the struck nucleon is balanced coherently by the residual nucleus [19, 20]. A second class of models [21, 4] assumes that the backward yield is due to rescattering processes in the nucleus of the incident and outgoing particles. These initial and final interactions include true π -absorption and Δ -rescattering in the intermediate states.

The results of our experiment that the ratio of backward going neutrons above a momentum of 0.32 GeV/c in coincidence with two high p_t protons, is substantially larger adds new information that has to be accommodated in the theoretical models. We speculate that the reason for the difference is the strong total center of mass (s) dependence of the hard reaction cross section and its sensitivity to the short range nucleon correlations in nuclei. The strong s dependence of the hard reaction (for example $1/s^{10}$ for pp elastic scattering) selectively chooses the high momentum protons in the nuclei. Those protons most likely have a correlated partner at short range which are the neutrons that dominate the backward going yield [17, 18, 13]. This speculation needs to be checked with detailed calculations.

We wish to thank Drs. L. Frankfurt M. Strikman and M. Sargsyan for their theoretical input. We are pleased to acknowledge the assistance of the AGS staff in building and rebuilding the detector and supporting the experiment, particularly our liaison engineers, J. Mills, D. Dayton, C. Pearson. We acknowledge the continuing support of D. Lowenstein and P. Pile. This research was supported by the U.S. - Israel Binational Science foundation,

the Israel Science Foundation founded by the Israel Academy of Sciences and Humanities, the NSF grants PHY-9501114, PHY-9722519 and the U.S. Department of Energy grant DEFG0290ER40553.

References

- [1] G.A. Leksin in Proceeding of the XVIII International conference on High Energy Physics, Tbilisi, 1976, ed. N. N. Bogolubov et al.
- [2] Yu D. Bayukov *et al.*, Sov. J. Nucl. Phys. 18 (1974) 639; Sov. J. Nucl. Phys. 42 (1985) 116, and 238; Sov. J. Nucl. Phys. 34 (1981) 437.
- [3] Yu D. Bayukov *et al.*, Sov. J. Nucl. Phys. 41 (1985) 101; ITEP-5-1985 (1985) 67.
- [4] V.I. Komarov *et al.*, Nucl. Phys. A326(1979)297.
- [5] K.V. Alanakyan *et al.*, Sov. J. Nucl. Phys. 25 (1977) 292.
- [6] J. P. Berge *et al.*, Phys. Rev. D18 (1978) 1367.
- [7] V.I. Efremenko *et al.*, Phys. Rev. D22 (1980) 2581.
- [8] E. Matsinos *et al.*, Z. Phys. C44 (1989) 79.
- [9] M.A. Shupe, *et al*, *EVA, a solenoidal detector for large angle exclusive reactions: Phase I - determining color transparency to 22 GeV/c*. Experiment E850 Proposal to Brookhaven National Laboratory, 1988 (unpublished).
- [10] S. Durrant, *Measurement of the dependence of the $C(p,2p)$ cross section on the transverse component of the spectral momentum*, PhD thesis, Pennsylvania State University, 1994 (unpublished).
- [11] Y. Mardor, *Quasi-Elastic Hadronic Scattering at Large Momentum Transfer*, PhD thesis, Tel Aviv University, 1997 (unpublished) and I.Mardor, *Nuclear filtering in wide angle exclusive scattering*, PhD thesis, Tel Aviv University, 1997 (unpublished).

- [12] J.Y. Wu *et al.*, Nuclear Instruments and Methods A 349 (1994) 183.
- [13] J. Aclander *et al.*, Phys. Lett. B453 (1999) 211.
- [14] R. Madey *et al.*, Nucl. Instr. and Meth. 214 (1983) 401.
- [15] R. Cecil, B.D. Anderson, R. Madey, Nucl. Inst. and Meth. 161, (1979) 439.
- [16] D. J. Hughes and R. B. Schwartz, BNL report 325 (1958).
- [17] L.L. Frankfurt and M.I. Strikman, Phys. Rep. 76 (1981) 214; *ibid*, 160 (1988) 235.
- [18] L.L. Frankfurt and M.I. Strikman, Phys. Lett. B69 (1977) 87.
- [19] S. Frankel, Phys. Rev. Lett. 38 (1977) 1338.
- [20] D. Amado and R.H. Woloshyn, Phys. Rev. Lett. 36 (1976) 1435.
- [21] V.B. Kopeliovich, Sov. J. Nucl. Phys. 26 (1977) 297.

Tables

Table 1

incident/ backward emitted particle	energy (GeV)	target	integration range (GeV/c)	integration range (Deg.)	Ref.	RATIO (%)
p/n	5.9	C	0.32-0.5	90-130	a	29.9±1.6
π /n	5.9	C	0.32-0.5	90-130	b	26.2±2.4
$\bar{\nu}$ /p	WB^c	Ne	0.2-0.7	90-180	d1	7±1
p/p	3.66	Ne	0.2-0.7	90-180	d2	8±3
$\bar{\nu}$ /p ν /p NC/p	WB^e	Ne	0.2-0.8	90-180	f	10±1 12±4 10±1
$\bar{\nu}$ /p ν /p	WB^e	Ne	0.35-0.8	90-180	g	6.0±0.2 8.5±0.3
p/p	0.64	C	0.311-0.54	90-180	h	6.0±1.5

a- This work. If we extrapolate to 180° under the assumptions in the text, we get a value of $(46.5\pm 2.5)\%$.

b- This work. If we extrapolate to 180° under the assumptions in the text, we get a value of $(40.8\pm 3.7)\%$.

c- A wide band $\bar{\nu}$ beam from 300 GeV/c incident protons.

d1- Results of ref. [6].

d2- Deduced in ref. [6] from measurements of ref. [2] to satisfy the same selection criteria as used in ref. [6].

e- A wide band $\bar{\nu}$ beam from 400 GeV/c incident protons.

f- "(BP+2BP)/TOTAL" from Table I of ref. [7]

g- "1 Backward proton rate" from Table 1 of ref. [8].

h- Integral of $I(\theta_3)$ from Table 2 divided by σ_t from ref. [4]

Figure captions.

Fig. 1 The set up of the neutron counter arrays. Only the magnet of the spectrometer is shown with the position of the targets. The lead shield and veto counters above the neutron counter arrays are not shown.

Fig. 2 Proton and pion induced neutron invariant momentum spectra. The vertical axis is $\ln[(E_n/p_n) \times \frac{N_3}{d(p_n^2)}]$, The horizontal axis is p_n^2 . E_n and p_n are the energy and momentum of the neutron. N_2 is the number of events with exactly two charged particles, each with $p_t > 0.6$ GeV/c, detected in the spectrometer. N_3 is the number of N_2 events that also have a single neutron entering the neutron counters. The neutron yield is corrected for the detection efficiency and attenuation. Above $p_n^2 > 0.1$ (GeV/c)² the points are fitted to a straight line to obtain the slope parameter defined in Eq. 1. The resulting slopes with the fitting errors are shown.

Fig. 3 The relative yield per solid angle $\frac{dN_3}{N_2 d\Omega_n}$ of backward going neutrons above 0.32 GeV/c as a function of the neutron angle. N_3 and N_2 are defined in Fig. 2 and the text. The data are for the proton and pion induced reactions. The lines represent fits to a constant which is used to estimate the total backward emission yield, see text.

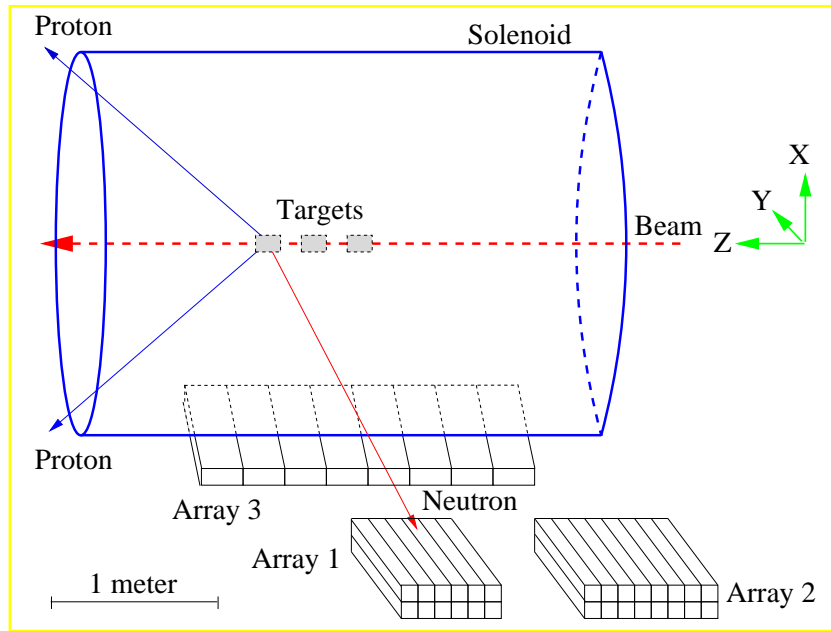


FIG 1

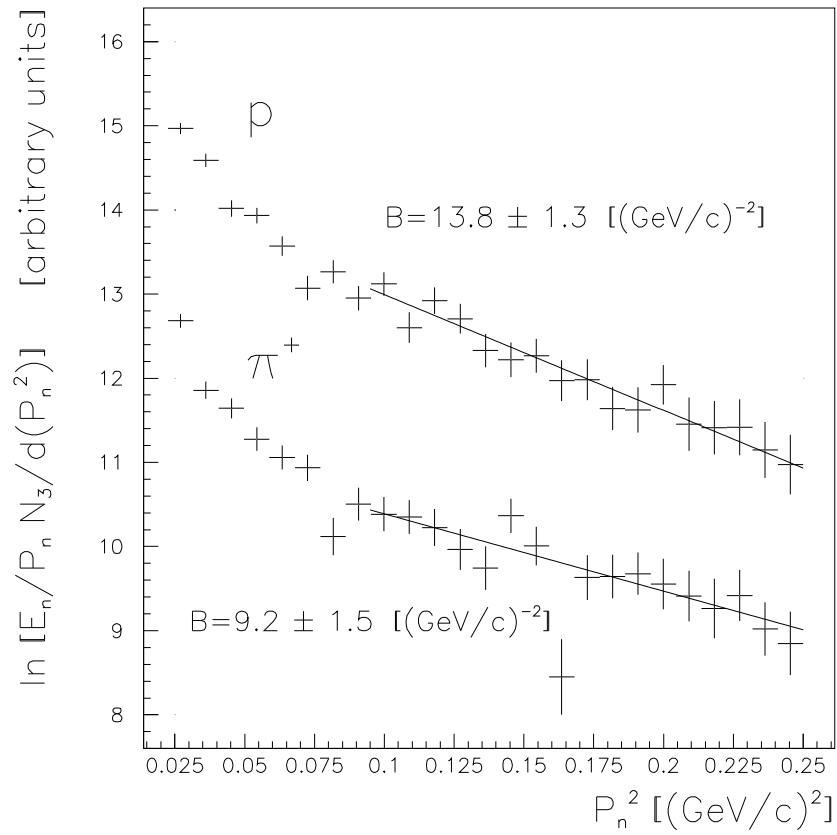


FIG 2

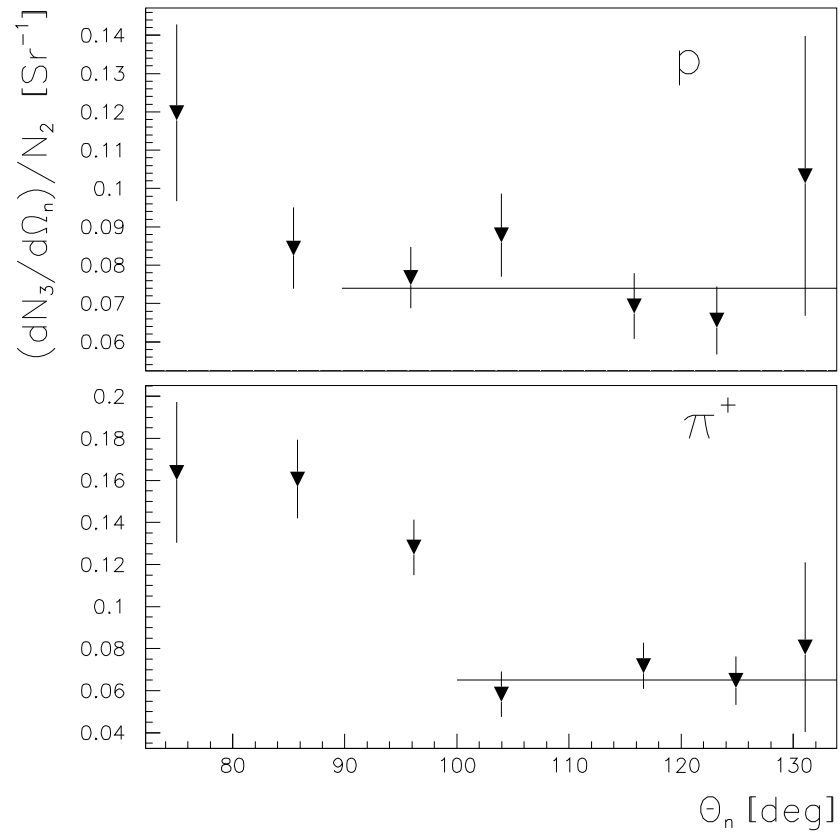


FIG 3